Journal of the American College of Cardiology
© 2004 by the American College of Cardiology Foundation
Published by Elsevier Inc.

Vol. 44, No. 11, 2004
ISSN 0735-1097/04/$30.00
doi:10.1016/j.jacc.2004.08.066

Inhibition of ErbB2 Causes Mitochondrial Dysfunction in Cardiomyocytes

Implications for Herceptin-Induced Cardiomyopathy

Luanda P. Grazette, MD, MPH,*† Wolfgang Boecker, MD,* Takashi Matsui, MD, PHD,*† Marc Semigran, MD,† Thomas L. Force, MD,‡ Roger J. Hajjar, MD,*† Anthony Rosenzweig, MD*†

Boston, Massachusetts

OBJECTIVES We investigated the effects of erbB2 inhibition by anti-erbB2 antibody on cardiomyocyte survival and mitochondrial function.

BACKGROUND ErbB2 is an important signal integrator for the epidermal growth factor family of receptor tyrosine kinases. Herceptin, an inhibitory antibody to the erbB2 receptor, is a potent chemotherapeutic but causes cardiac toxicity.

METHODS Primary cultures of neonatal rat ventricular myocytes were exposed to anti-erbB2 antibody (Ab) (7.5 μg/ml) for up to 24 h. Cell viability, mitochondrial function, and apoptosis were measured using multiple complementary techniques.

RESULTS ErbB2 inhibition was associated with a dramatic increase in expression of the pro-apoptotic Bcl-2 family protein Bcl-xS and decreased levels of anti-apoptotic Bcl-xL. There was a time-dependent increase in mitochondrial translocation and oligomerization of bcl-associated protein (BAX), as indicated by 1,6-bismaleimidohexane crosslinking. The BAX oligomerization was associated with cytochrome c release and caspase activation. These alterations induced mitochondrial dysfunction, a loss of mitochondrial membrane potential (ψ) (76.9 $\pm$ 2.4 vs. 51.7 $\pm$ 0.1; $p < 0.05$; $n = 4$), a 35% decline in adenosine triphosphate levels ($p < 0.05$), and a loss of redox capacity (0.72 $\pm$ 0.04 vs. 0.64 $\pm$ 0.02; $p< 0.01$). Restoration of Bcl-xL levels through transactivating regulatory protein-mediated protein transduction prevented the decline in ψ mitochondrial reductase activity and cytosolic adenosine triphosphate.

CONCLUSIONS Anti-erbB2 activates the mitochondrial apoptosis pathway through a previously undescribed modulation of Bcl-xL and -xS, causing impairment of mitochondrial function and integrity and disruption of cellular energetics. (J Am Coll Cardiol 2004;44:2231–8) © 2004 by the American College of Cardiology Foundation

ErbB2 is a member of the epidermal growth factor (EGF) family of tyrosine (Tyr) kinase receptors and is overexpressed at high levels in a variety of cancers (1). A monoclonal antibody to erbB2, Trastuzumab (Herceptin, Genentech Inc., San Francisco, California), has yielded significant improvements in response rate and survival in breast cancer treatment (2). Early experience with the agent has also been notable for cardiotoxicity and dramatic exacerbation of anthracycline-induced cardiomyopathy, with up to a 27% incidence of moderate to severe cardiac dysfunction (2,3). Whereas the erbB receptors and their high-affinity ligands, the neuregulins, have important roles in normal cardiac development (4), the basis of cardiac dysfunction after inhibition of this system remains unclear.

Recently, two studies utilizing cardiac-specific deletion of erbB2 demonstrated early cardiac dysfunction and severe dilated cardiomyopathy in the absence of readily demonstrable cardiomyocyte apoptosis (5,6). In both studies, erbB2 conditional mutants were born with phenotypically normal hearts but developed dilated cardiomyopathy as adults (5,6). Ozcelik et al. (6) saw no difference in apoptosis, as measured by terminal deoxynucleotidyl transferase dUTP nick end labeling (TUNEL) staining, between wild-type and conditional knockouts even after aortic banding. Their analysis suggested that erbB2 had a role in normal heart physiology but was not necessary for survival of cardiomyocytes (5,6). Crone et al. were also unable to detect any difference in TUNEL-positive cardiomyocytes but, using a highly sensitive polymerase chain reaction deoxyribonucleic acid (DNA) fragmentation assay, were able to detect increased DNA fragmentation in whole-ventricle samples from erbB2 conditional knockout mice (5). To test the functional significance of this potential low-level apoptosis, the investigators overexpressed the anti-apoptotic Bcl-2 family gene Bcl-xL. Expression of Bcl-xL resulted in partial rescue of chamber contractility and dilation (5). Whether this functional rescue was due to inhibition of apoptosis or other effects of Bcl-xL is unknown.

Even though the Bcl proteins were first recognized for their role in apoptosis, they also modulate mitochondrial homeostasis and integrity. In this study, we examined the effect of antibody-mediated erbB2 receptor antagonism on

From the *Program in Cardiovascular Gene Therapy, Cardiovascular Research Center, Boston, Massachusetts; †Cardiology Division, Massachusetts General Hospital, Harvard Medical School, Boston, Massachusetts; and ‡Tufts New England Medical Center, Boston, Massachusetts. This work has in part been supported by grants from the National Institutes of Health (HL-59521, HL-61557, HL-073363) to Dr. Rosenzweig, (HL-67716) to Dr. Grazette, (HL-04250) to Dr. Matsui, and (50361, 57623) to Dr. Hajjar. Dr. Böcker was supported by a Lilly Scholarship from the Deutsche Gesellschaft für Kardiologie-Herz und Kreisslaufforschung.

Manuscript received January 28, 2004; revised manuscript received August 10, 2004, accepted August 23, 2004.

Abbreviations and Acronyms

ARVM = adult rat ventricular myocytes
ATP = adenosine triphosphate
DNA = deoxyribonucleic acid
EGF = epidermal growth factor
MTT = mitochondrial reductase activity
NRVM = neonatal rat ventricular cardiomyocytes
PBS = phosphate-buffered saline
RNA = ribonucleic acid
TUNEL = terminal deoxynucleotidyl transferase dUTP nick end labeling
Tyr = tyrosine

mitochondrial integrity and function, death pathway signaling, and induction of apoptosis in rat cardiomyocytes. Here we show that anti-erbB2 has significant adverse effects on mitochondrial function and energetics. Further, we demonstrate that erbB2 inhibition is associated with a previously undescribed alteration in the expression and ratio of the antagonistic Bcl-2 family proteins Bcl-xL and -xS. This shift in the apoptotic threshold leads to mitochondrial dysfunction and caspase activation.

MATERIALS AND METHODS

Cardiomyocyte isolation and experimental design. Neonatal rat ventricular cardiomyocytes (NRVM) were prepared from the hearts of Sprague-Dawley pups as previously described (7). We tested multiple antibodies and selected mAb clone 9G6 (Oncogene, Cambridge, Massachusetts) as the inhibitory antibody used throughout these studies based on its ability to bind the rat receptor (8) and to inhibit receptor kinase activity (9), as well as its ability to inhibit receptor phosphorylation in rat cardiomyocytes (data not shown). Three days after plating cells in Dulbecco's modified eagle medium with 5% fetal calf serum, 1% penicillin/streptomycin were treated with anti-erbB2 Ab (clone 9G6) or an isotype-matched control antibody (clone 122-25) (control Ab) (Oncogene, Cambridge, Massachusetts) at concentrations from 5 to 7.5 μg/ml. To confirm the functional role of Bcl-xL, a cell-permeable peptide containing the N-terminal homology domain (BH4) linked to carrier peptide human immunodeficiency virus (HIV)-TAT (TAT-BH4, Calbiochem, San Diego, California) (200 nM) was added to NRVM 1 h before anti-erbB-2 Ab for selected experiments.

Adult rat ventricular myocytes (ARVM) preparation. Adult rat ventricular myocytes were isolated and cultured from hearts excised from deeply anesthetized Sprague-Dawley rats as has been previously described (10,11). Adult rat ventricular myocytes were treated immediately after plating with anti-erbB-2 Ab or the isotype control Ab at concentrations of 5 to 7.5 μg/ml.

Ribonucleic acid (RNA) interference. Neonatal rat ventricular cardiomyocytes were transfected with a 21-base-pair double-stranded RNA duplex targeted to a sequence within the open reading frame of RNNEUR, the rodent erbB2 gene (AAGUGUGUACCGGCACAGACA) (Dharmacon Research, Lafayette, Colorado). Sterile RNase-free water was added to the duplexed and desalted complex to generate 20-μM duplex siRNA in annealing buffer. Each 60 mm plate was transfected with 30 μl of 20-μM, annealed duplex. The duplex siRNA was added to Transit-TKO transfection reagent and serum-free Dulbecco's modified eagle medium. After a 15-min incubation at room temperature, the mixture was added to culture plates and incubated for 24 h. Cells were analyzed for gene silencing at 48 and 72 h.

Cell fractionation. Neonatal rat ventricular cardiomyocytes were washed twice with cold phosphate-buffered saline (PBS), collected and resuspended in an isotonic buffer containing Hepes pH 7.5, 20 mM, Sucrose 250 mM, NaCl 10mM, 1.5mM MgCl2, EGTA 1 mM, EDTA 1 mM with protease inhibitors. After 30 min on ice, cells were mechanically disrupted and centrifuged (750 *g* for 10 min) to pellet un-lysed cells and nuclei. Supernatants were collected and centrifuged at 16,000 *g* for 20 min to pellet the mitochondria-rich heavy membrane fraction. The supernatant (cytosolic fraction) was removed and the heavy membrane pellet was suspended in lysis buffer supplemented with 1% triton. Protein concentrations of the fractions were equalized, and sodium dodecyl sulfate sample buffer was added to a final concentration of 1X.

BMH crosslinking. To detect BAX homo-oligomerization, the irreversible cross-linker 1,6-bismaleimidohexane was obtained from Pierce (Rockford, Illinois). A 10-mM stock solution in dimethyl sulfoxide was added to mitochondrial fractions at a 1:11. Crosslinking took place for 30 min at room temperature, followed by centrifugation to pellet mitochondria.

Immunoblot analysis. Protein extraction and immunoblotting was performed as previously described (7). Cell lysates were matched for protein concentration and were then separated by sodium dodecyl sulfate-polyacrylamide gel electrophoresis and transferred to Hybond-C extra (Amersham Pharmacia Biotech, Buckinghamshire, United Kingdom).

Primary antibodies were used to the following: BAD, Bcl-xL, and BAX (Santa Cruz Biotechnology Inc.), phospho-erbB2 (originally raised to human Tyr-877, which corresponds to and cross-reacts with rat phospho-Tyr882, as an indicator of receptor activation), erbB2 (9G6, as an inhibitory antibody), caspase 9, cleaved caspase 9, caspase 3, cleaved caspase 3, phosphor-bcl-2 (Ser-70), phospho-bad (Ser-112, Ser-136) (New England Biolabs Inc.), cytochrome c (Pharmingen, San Diego, California), and cytochrome oxidase IV (Molecular Probes, Eugene, Oregon), all at 1:1000.

Cytochrome c quantitative sandwich enzyme immunoassay. Neonatal rat ventricular cardiomyocytes were cultured in 12-well plates at a density of 500,000/well. Twenty-four hours after treatment, cells were collected and fractionated as described and cytosolic cytochrome c was measured using

the Quantikine M rat/mouse cytochrome c immunoassay according to the manufacturer's directions. Cytosolic fractions were pipetted in triplicate onto a microplate precoated with rat/mouse cytochrome c. After a 2-h incubation and washing, substrate solution was added to each well. The reaction was stopped after 30 min and the optical density was measured at 540 using the Wallac Victor2 1420 Multilable Counter (Perkin Elmer, Boston, Massachusetts).

Mitochondrial reductase activity (MTT). Mitochondrial reductase activity was measured in 96 well plates using the TACS MTT Assay (R&D, Minneapolis, Minnesota) according to the manufacturer's protocol. Mitochondrial reductase activity (3-[4, 5-dimethylthiazol-2-yl]-2, 5-diphenyltetrazolium bromide), which is reduced to an insoluble formazan dye in metabolically active cells, was added 4 h before assay. Absorbance was measured at 595 using the Biorad 3550 microplate reader.

Viability/cytotoxicity. Neonatal rat ventricular cardiomyocytes in 96-well flat bottom plates were cultured as described. Quantification of live versus dead cells was achieved simultaneously using calcein AM (Molecular Probes), which is well retained and fluoresces green (ex/em 495/515) in living cells and ethidium homodimer (Molecular Probes), which enters damaged membranes and undergoes enhanced red fluorescence (ex/em 495/635) upon binding to nucleic acids. Fluorescence was measured using the Wallac Victor2 1420 Multilable Counter.

Change in mitochondrial membrane potential (ψ). The mitochondrial selective dye MitoTracker Red (Molecular Probes) was used to label cells for flow cytometry. At 24 h the MitoTracker probe was added to NRVM at 100-nM final concentration. Cells were incubated for 15 min at 37°C, washed with PBS, and fixed in 3% paraformaldehyde. Flow cytometry was performed using a Becton Dickinson FACSCAN. Data were collected by Cellquest software and analyzed with Cellfit software.

Measurement of adenosine triphosphate (ATP) concentration. Neonatal rat ventricular cardiomyocytes were cultured in white 96-well flat-bottom plates at a density of 30,000/well. Adenosine triphosphate content was measured using the Apoglow (Cambrex, East Rutherford, New Jersey) luciferin-luciferase bioluminescence kit following the manufacturer's protocol.

DNA end labeling (TUNEL). For in situ detection of apoptosis in individual cells, TUNEL staining was performed using the MEBSTAIN Apoptosis Kit Direct according to the manufacturer's recommendations. Cardiomyocytes were identified by simultaneous immunostaining with the anti–sarcomeric-actinin monoclonal Ab (EA-53, Sigma, St. Louis, Missouri) labeled with Cy3 tagged goat antimouse immunoglobulin G secondary Ab (Sigma). For quantification of the number of apoptotic cardiomyocytes, nuclei were counterstained with Hoechst 33258 (Sigma) and the total numbers of nuclei and TUNEL-positive nuclei were counted in −actinin-positive cells in 8 to 10 low-power fields in three independent experiments. More than 1,500 nuclei were counted for each condition.

DNA fragmentation (DNA laddering). The DNA laddering was performed as previously described (7): 1 μg DNA from each sample was labeled with 0.5 μCi [$-^{32}$P] dCTP (DuPont NEN, Boston, Massachusetts) in the presence of 5 U of Klenow polymerase. The reaction was terminated (10-mmol/l EDTA, 75°C for 10 min) and subjected to 1.8% agarose gel electrophoresis and autoradiography.

Propidium iodide flow cytometry. Cells were fixed with 70% ethanol/PBS, washed with PBS, and resuspended in PBS with propidium iodide 20 μg/ml and RNase type IIa (Sigma). Analyses were performed using a Becton Dickinson FACSCAN. Gating was performed to exclude small debris. The hypo-diploid population of cells was considered apoptotic. Data were analyzed by Cellfit software. Results shown are from eight independent experiments.

Statistical analysis. Statistical analysis was carried out using the Prism software package (Graphpad, San Diego, California). Comparisons between groups were made using analysis of variance followed by Student-Newman-Keuls multiple-comparisons post-testing. Significance was accepted at a value of $p < 0.05$. Values are expressed as the arithmetic mean ± SEM.

RESULTS

Inhibition of erbB2. We tested multiple antibodies to identify an appropriate inhibitory antibody for use with rat cardiomyocytes. MAb clone 9G6 inhibits erbB2 tyrosine kinase activity in human cell lines (9) and cross-reacts with the rat receptor homologue (8). Phosphorylation of the rat erbB2 receptor at Tyr882 appears necessary for full receptor activation and mitogenesis (12). Using a phosphospecific antibody corresponding to this site, we saw ~40% decline in receptor phosphorylation in cultured cardiomyocytes treated with mAb 9G6 compared with untreated or isotype-matched control Ab-treated cells (data not shown). For these reasons, mAb 9G6 was used as the inhibitory anti-erbB2 mAb throughout these studies.

Alteration in Bcl-x expression. ErbB2 inhibition was associated with a dramatic increase in expression of Bcl-xS, which was generally not detectable in cardiomyocytes at baseline. In contrast, expression of Bcl-xL, which was robust in untreated cardiomyocytes, decreased substantially over 24 h of anti-erbB2 treatment (Fig. 1A). To confirm that these effects were specifically due to erbB2 inhibition, we also used RNA interference to reduce erbB2 receptor expression. Ribonucleic acid interference to erbB2 substantially reduced erbB2 expression and mediated changes in Bcl-xL and -xS expression similar to those seen with antibody treatment (Fig. 1B). Thus, loss of erbB2 function, whether through antibody blockade or reduced expression, dramatically perturbs the ratio of Bcl-xL to -xS in favor of the latter.

JACC Vol. 44, No. 11, 2004
December 7, 2004:2231–8

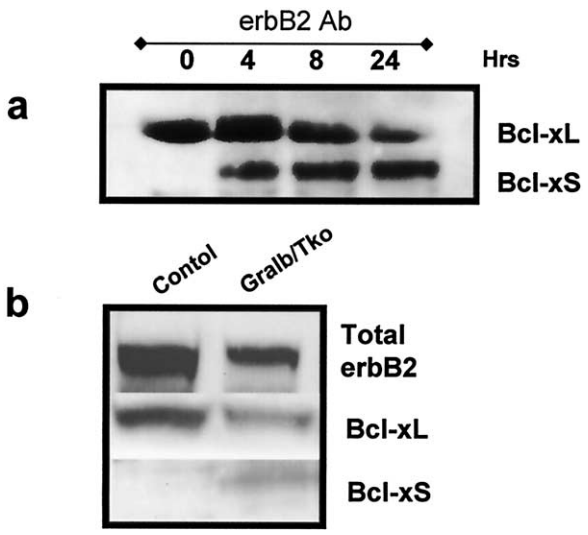

Figure 1. Effects of erbB2 inhibition on Bcl-xL and -xS expression. **(a)** ErbB2 inhibition was associated with an increase in expression of Bcl-xS and decreased expression of Bcl-xL in a time-dependent manner. Western blot shown is representative of five independent experiments. **(b)** A 21-base-pair double-stranded ribonucleic acid sequence corresponding to a section within the open reading frame of the rodent erbB2 gene (Gralb) was solubilized in TransIT-TKO (Mirus Research Solutions, Houston, Texas) for transfection of cardiomyocytes. Reduced expression of erbB2 and altered Bcl-x expression were seen 48 h after transfection. Western blots representative of four independent experiments.

Activation of mitochondrial death signaling. We next examined whether the observed alterations in Bcl protein expression led to activation of mitochondrial apoptotic signaling, as has been previously reported in other cell types (13). Anti-erbB2 induced a time-dependent increase in the protein level of BAX (Fig. 2A). There was also increased oligomerization of BAX within the mitochondria-rich heavy membrane fraction (HM) (Fig. 2B). Homo-oligomerization of BAX, as demonstrated by BMH crosslinking, has been shown to precede release of cytochrome c (14). We observed depletion of cytochrome c from the mitochondrial fraction, in a time-dependent fashion, beginning at 8 h after anti-erbB2 treatment (Fig. 2C, upper). Cytochrome c reached detectable levels in the cytosolic fraction at 24 h as measured by cytochrome c ELISA (control, 0.47 ± 0.05 and control Ab, 0.6 ± 0.11 vs. anti-erbB2 1.3 ± 0.09, n = 3, $p < 0.05$). Cleavage and activation of caspase 9, an initiator caspase in the mitochondrial pathway, also increased in a time-dependent manner beginning at 16 h (Fig. 2D, lower). Cleavage of caspase 3, a downstream target of caspase 9 and important effector caspase, was also documented by Western blotting (Fig. 2E, middle) and by caspase 3 activity assay (6,794 ± 390 vs. 7,628 ± 481, p = 0.05)

There were no significant changes in expression or localization observed for Bcl-2, phospho-Bcl-2, BAD, or phospho-BAD (data not shown).

Adult cardiomyocytes. We also examined whether the downstream signaling consequences of anti-erbB2 could be extended to adult rat cardiomyocytes. Anti-erbB2 treatment resulted in a marked increase in expression of Bcl-xS and a moderate increase in Bcl-xL, resulting in a net increase in the Bcl-xS/Bcl-xL ratio and an increase in BAX (Fig. 3A). As with neonatal cardiomyocytes, this elevated Bcl-xS/Bcl-xL and elevation in BAX was associated with an increase in cytosolic cytochrome c (Fig. 3B).

Mitochondrial membrane potential (ψ). Because Bcl-xL has been reported to have an important role in maintaining both mitochondrial membrane potential and adenosine

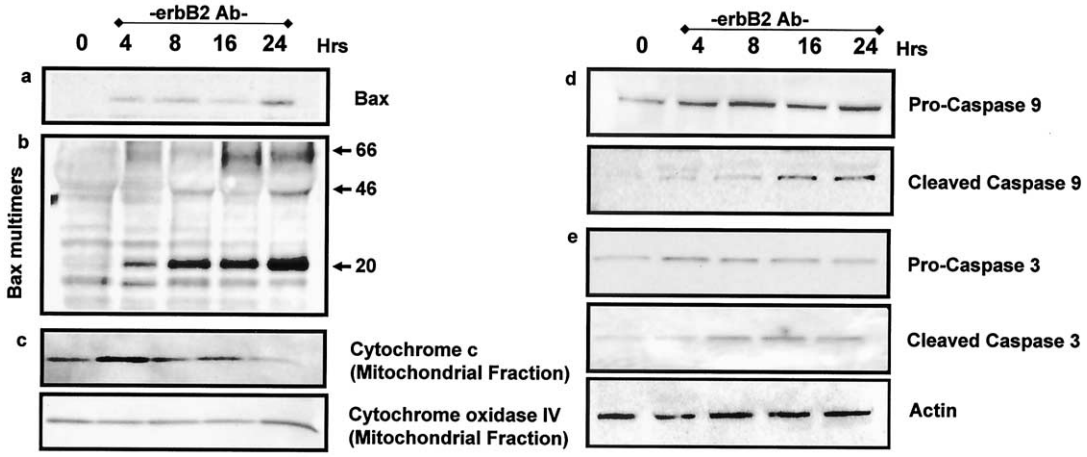

Figure 2. Activation of mitochondrial death agonists. Neonatal rat ventricular cardiomyocytes were exposed to anti-erbB2 antibody (erbB2 Ab) for the specified times. Lysates were collected and separated by electrophoresis under denaturing conditions with protein detection by immunoblotting following sodium dodecyl sulfate-polyacrylamide gel electrophoresis. **(a)** Time-dependent increase in expression of bcl-associated protein. **(b)** Treated cells were subjected to subcellular fractionation to yield a mitochondria rich heavy membrane fraction (HM). The HM was incubated for 30 min with the irreversible crosslinker BMH. Immunoblot demonstrates crosslinked BAX multimers. **(c) (Upper panel)** Depletion of cytochrome c from the mitochondrial fraction, beginning at 8 hours after anti-erbB2 treatment. **(Lower panel)** Cytochrome oxidase used for control of mitochondrial protein loading. **(d)** Anti-erbB2 induced a time-dependent increase in cleavage and activation of caspase 9 beginning at 16 h. **(e)** Increase cleavage and activation of caspase 3 were also observed beginning as early as 8 h after treatment. **(Bottom panel)** Actin immunoblotting to control for cytosolic protein loading. All Western blots shown are representative of three or more independent experiments.

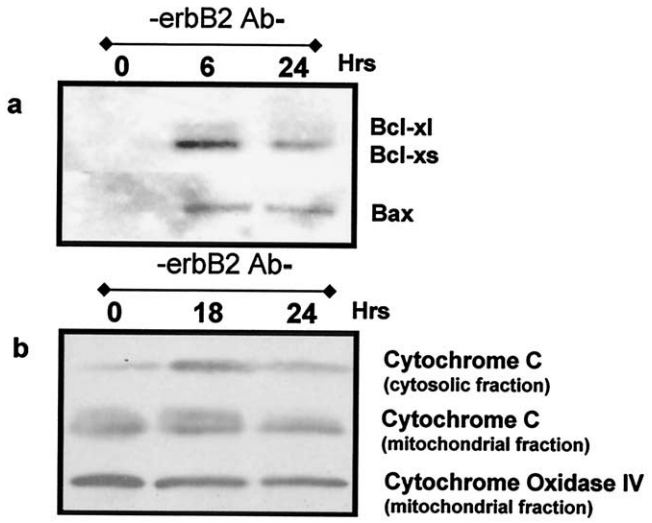

Figure 3. Anti-erbB2 effects in adult rat ventricular myocytes. Adult rat ventricular myocytes were exposed to anti-erbB2 antibody (Ab) for the specified times. Lysates were collected, separated by electrophoresis, and immunoblotted. **(a)** ErbB2 inhibition was associated with an increase in expression of Bcl-xS and Bcl-xL. **(b)** Cytochrome c release into the cytosol. Bax = bcl-associated protein.

diphosphate/ATP exchange, we investigated the effect of anti-erbB2 on these parameters (15,16). We initially used the mitochondrial potential sensor Mitotracker red to evaluate the mitochondrial membrane potential (ψ). Using flow cytometry, we observed a 25% ($p < 0.05$) decrease in red fluorescence in anti-erbB2–treated cells compared with controls (Fig. 4A).

Intracellular ATP. To investigate whether these alterations in mitochondrial integrity were sufficient to interfere with cellular energetics, we compared the intracellular ATP reserves of anti-erbB2, control Ab, and control untreated cells. There was a substantial decrease in ATP-generated luminescence in anti-erbB2-treated cells compared with untreated cells (35% reduction, 847 ± 75 vs. 1,297 ± 112 cps, $p < 0.01$) or control antibody-treated cells (25% decrease, 847 ± 75 vs. 1,131 ± 77.2 cps, $p < 0.05$) (Fig. 4B).

ErbB-2 inhibition induces a loss of redox capacity in neonatal cardiomyocytes. Reduction of the tetrazolium compound MTT is dependent upon the presence of nicotinamide adenine dinucleotide and nicotinamide adenine dinucleotide phosphate, as well as intact mitochondrial electron transport. In cardiomyocytes reduction of MTT occurs primarily at the mitochondria and therefore reflects mitochondrial function and metabolic activity of cardiomyocytes. We found that erbB2 inhibition reduced mitochondrial reductase activity in cells exposed to anti-erbB2 for 24 h by 20% compared with untreated and isotype-matched antibody-treated controls (0.804 vs. 1.0, $p < 0.05$, normalized data) (Fig. 4C). To examine whether these changes were due to a decline in cell number, we performed calcein AM/ethidium homodimer vital staining in parallel with MTT and saw no change across treatment groups.

Similar to NRVM, there was an approximate 18% decline in redox activity as measured by MTT in anti-erbB-2 treated compared with untreated and control Ab-treated ARVM (0.076 ± 0.005 vs. 0.062 ± 0.002, $p < 0.01$).

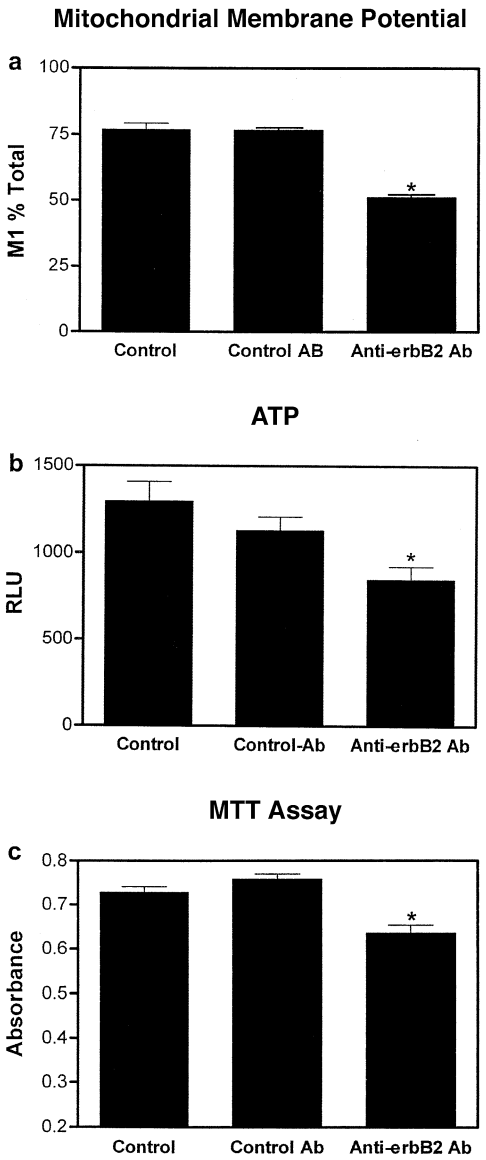

Figure 4. Anti-erbB2 reduces mitochondrial membrane potential adenosine triphosphate (ATP) concentration and redox capacity in neonatal rat ventricular cardiomyocytes. Neonatal rat ventricular cardiomyocytes were stained with a fluorescent probe selective for metabolically active mitochondria Mitotracker red. **(a)** Results of flow cytometry of cells stained with Mitotracker red dye. Anti-erbB2 treatment resulted in decreased red fluorescence (76.85 ± 2.4 vs. 51.1 ± 0.072, *$p < 0.05$, n = 4 independent experiments). **(b)** ATP content was measured using luciferin-luciferase bioluminescence. There was a 35% decrease in ATP content of anti-erbB2-treated cells at 36 h compared to untreated cells. Results, expressed as relative light units, are from three independent experiments with six replicates/condition (1,297 ± 112 vs. 847 ± 75, *$p < 0.01$). **(c)** Reduction of the tetrazolium salt mitochondrial reductase activity (MTT) to a corresponding formazan is an indicator of redox capacity. Redox capacity was quantified using a spectrophotometer at a wavelength of 590. Reported results represent pooled data from nine independent experiments with three or more replicates, for each condition reported, in each experiment (1.0 vs. 0.804, *$p < 0.01$: normalized data pooled from nine independent experiments, three replicates/condition). Ab = antibody; M1% = percent positive of gated cells.

JACC Vol. 44, No. 11, 2004
December 7, 2004:2231–8

BH4-TAT prevents anti-erbB2-induced mitochondrial dysfunction. Bcl-xL, a close homologue of Bcl-2, promotes cell survival. Anti-apoptotic Bcl-2 family members share sequence homology at multiple regions of the four Bcl-2 homology (BH) domains, however BH4 is the only domain conserved among all of the anti-apoptotic Bcl-2 proteins. The BH4 domain has been demonstrated to be necessary for binding to BAX (17), and deletion of the BH4 domain abrogates the anti-apoptotic activity of both Bcl-2 and -xL (13). It has been previously demonstrated that the conserved N-terminal region (BH4 domain) is both necessary and sufficient for prevention of apoptotic mitochondrial changes (13). To confirm the functional significance of reduced Bcl-xL expression in this setting, we used a cell-permeable peptide containing BH4 domain of Bcl-xL linked to the protein transduction domain of HIV-1, HIV-TAT. The cell-permeable Bcl-xL peptide completely prevented the decline in mitochondrial membrane potential, MTT activity, and intracellular ATP (Fig. 5). Thus, the observed reduction in Bcl-xL relative to Bcl-xS plays a critical role in mediating mitochondrial dysfunction after erbB2 inhibition.

ErbB-2 inhibition and apoptosis. To determine whether these changes in mitochondrial function and Bcl protein expression and mitochondrial apoptotic signaling induced increased apoptosis in NRVMs, we utilized propidium iodide flow cytometry, TUNEL staining, and DNA laddering in parallel. Surprisingly, despite upstream activation of the mitochondrial death pathway, there was only a modest increase in apoptosis as measured by TUNEL staining (6.5 $\pm$ 0.7% vs. 3.1 $\pm$ 0.4%, $p < 0.05$) (Figs. 6A and 6C) and flow cytometry of propidium iodide-labeled NRVM (8.3 $\pm$ 0.9% vs. 4.5 $\pm$ 0.6%, $p < 0.01$) (Fig. 6B). There was no discernible increase in DNA laddering (Fig. 6C). Although DNA laddering is highly specific, it is relatively insensitive to low-level apoptosis, and this likely accounts for the absence of DNA laddering in our samples (18).

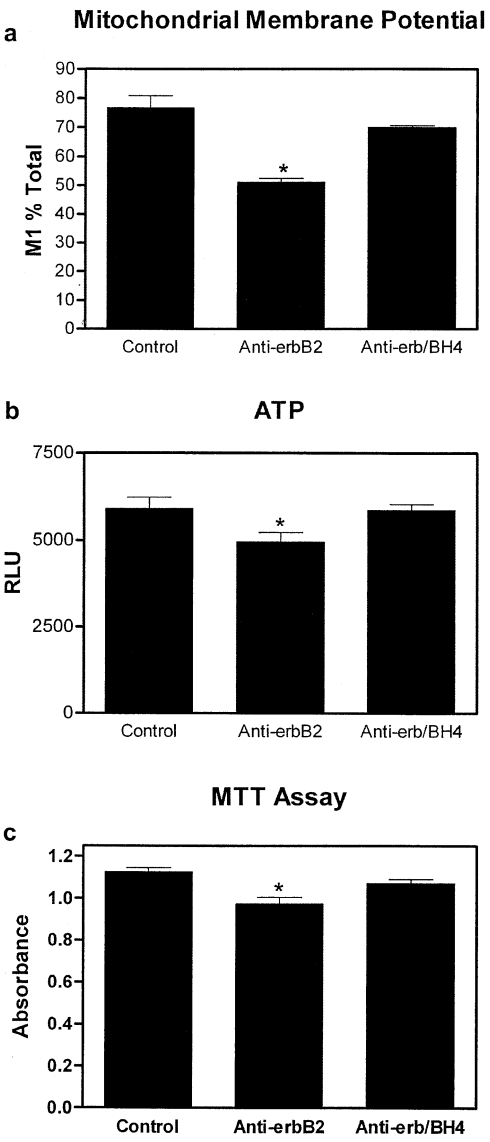

Figure 5. Transduction of TAT-BH4. To assess the functional significance of reduced Bcl-xL expression, cardiomyocytes were pretreated with a cell permeable Bcl-xL peptide (TAT-BH4). TAT-BH4 completely prevented the decline in **(a)** mitochondrial membrane potential (70 $\pm$ 0.57 vs. 51.2 $\pm$ 1.26, $^*p < 0.01$, n = 4 independent experiments), **(b)** intracellular adenosine triphosphate (5867 $\pm$ 166 vs. 4946 $\pm$ 272 relative light units, $^*p < 0.01$, n = 5 independent experiments), and **(c)** MTT activity (1.070 $\pm$ 0.02 vs. 0.9744 $\pm$ 0.03, $^*p < 0.05$, n = 5 independent experiments). Abbreviations as in Figure 4.

DISCUSSION

The erbB2 receptor is recognized as an oncogene in an increasing variety of cancers including gastric, endometrial, and lung. The expansion of erbB2 inhibition as an important chemotherapeutic modality is certain. However, early trial experience with a monoclonal antibody to erbB2, Trastuzumab (Herceptin), was notable for up to a 27% incidence of moderate to severe cardiac dysfunction (2,3). Whereas the most severe cardiomyopathy occurred when trastuzumab was combined with doxorubicin, Trastuzumab also caused significant cardiotoxicity when used in combination with paclitaxel and as monotherapy (2,3). Although 79% of the patients who developed cardiomyopathy in the trastuzumab trials experienced symptomatic improvement with conventional CHF therapy, the long-term consequences of exposure are unknown (3). A more complete understanding of erbB2 signaling in the heart therefore has dual relevance. First, as a potentially vital signaling mechanism controlling cardiomyocyte viability, and second as a means of identifying potential novel therapeutic targets that could be used to mitigate anti-erbB2-associated toxicity.

In this study, we provide a potential contributing mechanism for anti-erbB2-associated cardiac toxicity. Antibody-mediated inhibition of erbB2 was associated with dramatic alterations in the ratio of Bcl-xL/Bcl-xS, activation of BAX, and significant mitochondrial dysfunction. Human immunodeficiency virus TAT-mediated transduction of the conserved BH4 Bcl-xL domain prevented mitochondrial dys-

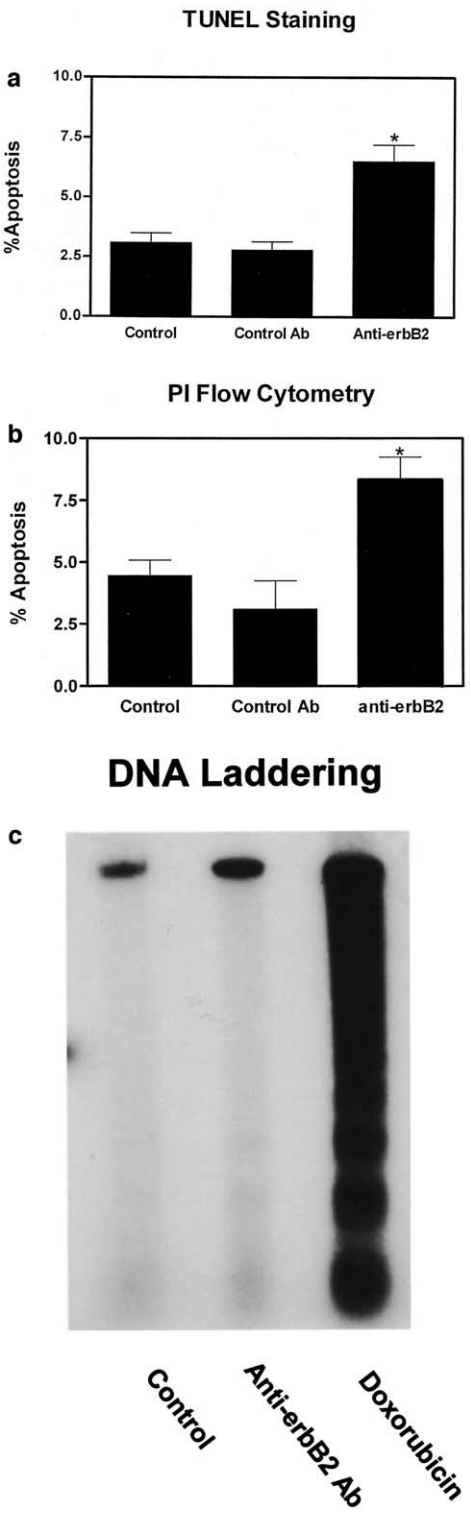

Figure 6. Apoptosis. **(a)** Anti-erbB2 increased apoptosis as measured by terminal deoxynucleotidyl transferase dUTP nick end labeling (TUNEL) (6.5 ± 0.7% vs. 3.1 ± 0.4%, *$p < 0.05$, n = 5 independent experiments). **(b)** Propidium iodide flow cytometry. Control, anti-erbB2, and control antibody (control Ab)-treated cells were fixed in ethanol and stained with PI. Anti-erbB2 increased the percentage of apoptotic cells. (8.3 ± 0.9% vs. 4.5 ± 0.6%, *$p < 0.01$, n = 8 independent experiments). **(c)** Deoxyribonucleic acid (DNA) laddering. DNA was collected from untreated, anti-erbB2, and doxorubicin (positive control)-treated cells, radiolabeled as described in Methods, and subjected to 1.8% agarose gel electrophoresis and autoradiography.

function, thus demonstrating the functional importance of this alteration.

Bcl-2 family proteins, first recognized as central integrators of death signaling, also play a closely related role in the regulation of mitochondrial stability and function (19). Activation of BAX and loss of mitochondrial membrane integrity is associated with multiple major deleterious intracellular consequences including loss of electron transport, generation of free radicals, release of pro-apoptotic proteins such as cytochrome c, and the uncoupling of oxidative phosphorylation so that ATP is hydrolyzed rather than synthesized (20–22). A recent report also establishes a central role for BAX in intracellular calcium cycling (23). Given the high energy requirements of cardiomyocytes, it is likely that mitochondrial dysfunction and a reduction in ATP stores ultimately result in compromised cardiac function. In fact, several studies have documented that agents that interfere with mitochondrial energetics have a negative impact on cardiac contractility in vitro and in vivo (24,25). Inhibition of oxidative phosphorylation, as occurs in anoxia or ischemia, leads to impairment or cessation of normal heart function in animal models (26). Further, in ischemia-reperfusion there is growing evidence that mitochondrial permeability transition pore (MPTP) opening is critical to the transition from reversible to irreversible reperfusion injury (26). It has also been demonstrated that MPTP opening is not irreversible and that the extent of mitochondrial re-closure correlates with functional recovery (26–28).

If opening of the MPTP also plays an important role in anti-erbB2 mediated myocyte injury, inhibitors of pore opening, such as Bcl-xL, should offer protection. In our model, transduction of the BH4 Bcl-xL domain prevented the reduction in ATP and mitochondrial dysfunction associated with erbB2 inhibition. Thus, rescue of mitochondrial dysfunction by Bcl-xL may provide an alternative mechanism by which overexpression of Bcl-xL ameliorates the cardiomyopathy seen in erbB2-targeted mice, even in the absence of considerable apoptosis (5,6,29). Therapeutic interventions that inhibit or reverse MPTP opening may prove useful in providing protection from apoptotic stimuli and potentially reversing diminished myocellular function.

Early investigations of neuregulin erbB signaling demonstrated that neuregulin inhibited apoptosis after serum deprivation (30). After inhibition of erbB2, which is essential in neuregulin signaling, we observed activation of upstream apoptotic signaling. We also observed a statistically significant increase in apoptosis, although the absolute degree of apoptosis was less than is generally seen with other pathophysiologically relevant stimuli (7). Chronic apoptosis, however, even at low levels, can contribute to loss of ventricular function and therefore cannot be ruled out as a contributing mechanism to trastuzumab-induced cardiomyopathy using this in vitro model (31). The present study, however, suggests that consequences of incomplete progression to apoptosis, such as mitochondrial dysfunction, likely also play a role. Several studies have previously demon-

strated partial activation of apoptotic programs in hibernating (32) and failing myocardium (33,34). Although the functional relevance and underlying mechanism of this "interrupted apoptosis" remain unclear, it is reasonable to hypothesize that such cardiomyocytes may be functionally impaired and more susceptible to additional apoptotic stimuli. This increased susceptibility could account for the potentiation of cardiotoxicity observed with erbB2 inhibition in the clinical arena. Importantly, incomplete initiation of apoptosis with diminished myocellular function might offer opportunities for reverse remodeling and therapeutic intervention. Recognition of mitochondrial dysfunction as a potential contributor to the cardiac dysfunction observed with erbB2 inhibition, even in the absence of overt apoptosis, may therefore broaden the therapeutic approaches being considered in this setting.

Acknowledgments

The authors thank Drs. Bruce Chabner and Syed Haq for their careful reading and invaluable input to this manuscript.

Reprint requests and correspondence: Dr. Anthony Rosenzweig, Massachusetts General Hospital, 114 16th Street, Room 2600, Charlestown, Massachusetts 02129. E-mail: arosenzweig@partners.org.

REFERENCES

1. Pegram M, Slamon D. Biological rationale for HER2/neu (c-erbB2) as a target for monoclonal antibody therapy. Semin Oncol 2000;27:13–9.
2. Slamon DJ, Leyland-Jones B, Shak S, et al. Use of chemotherapy plus a monoclonal antibody against HER2 for metastatic breast cancer that overexpresses HER2. N Engl J Med 2001;344:783–92.
3. Keefe D. Trastuzumab-associated cardiotoxicity. Cancer 2002;95:1592–600.
4. Carraway KL 3rd. Involvement of the neuregulins and their receptors in cardiac and neural development. Bioessays 1996;18:263–6.
5. Crone SA, Zhao YY, Fan L, et al. ErbB2 is essential in the prevention of dilated cardiomyopathy. Nat Med 2002;8:459–65.
6. Ozcelik C, Erdmann B, Pilz B, et al. Conditional mutation of the ErbB2 (HER2) receptor in cardiomyocytes leads to dilated cardiomyopathy. Proc Natl Acad Sci USA 2002;99:8880–5.
7. Matsui T, Li L, del Monte F, et al. Adenoviral gene transfer of activated phosphatidylinositol 3′-kinase and Akt inhibits apoptosis of hypoxic cardiomyocytes in vitro. Circulation 1999;100:2373–9.
8. Anton ES, Marchionni MA, Lee KF, Rakic P. Role of GGF/neuregulin signaling in interactions between migrating neurons and radial glia in the developing cerebral cortex. Development 1997;124:3501–10.
9. van Leeuwen F, van de Vijver MJ, Lomans J, et al. Mutation of the human neu protein facilitates down-modulation by monoclonal antibodies. Oncogene 1990;5:497–503.
10. Nagata K, Ye C, Jain M, Milstone DS, Liao R, Mortensen RM. Galpha(i2) but not Galpha(i3) is required for muscarinic inhibition of contractility and calcium currents in adult cardiomyocytes. Circ Res 2000;87:903–9.
11. Ren J, Gintant GA, Miller RE, Davidoff AJ. High extracellular glucose impairs cardiac E-C coupling in a glycosylation-dependent manner. Am J Physiol 1997;273:H2876–83.
12. Zhang HT, O'Rourke DM, Zhao H, et al. Absence of autophosphorylation site Y882 in the p185neu oncogene product correlates with a reduction of transforming potential. Oncogene 1998;16:2835–42.
13. Sugioka R, Shimizu S, Funatsu T, et al. BH4-domain peptide from Bcl-xL exerts anti-apoptotic activity in vivo. Oncogene 2003;22:8432–40.
14. Letai A, Bassik MC, Walensky LD, Sorcinelli MD, Weiler S, Korsmeyer SJ. Distinct BH3 domains either sensitize or activate mitochondrial apoptosis, serving as prototype cancer therapeutics. Cancer Cell 2002;2:183–92.
15. Vander Heiden MG, Chandel NS, Schumacker PT, Thompson CB. Bcl-xL prevents cell death following growth factor withdrawal by facilitating mitochondrial ATP/ADP exchange. Mol Cell 1999;3:159–67.
16. Vander Heiden MG, Li XX, Gottleib E, Hill RB, Thompson CB, Colombini M. Bcl-xL promotes the open configuration of the voltage-dependent anion channel and metabolite passage through the outer mitochondrial membrane. J Biol Chem 2001;276:19414–9.
17. Hirotani M, Zhang Y, Fujita N, Naito M, Tsuruo T. NH2-terminal BH4 domain of Bcl-2 is functional for heterodimerization with Bax and inhibition of apoptosis. J Biol Chem 1999;274:20415–20.
18. Lesauskaite V, Epistolato MC, Ivanoviene L, Tanganelli P. Apoptosis of cardiomyocytes in explanted and transplanted hearts. Comparison of results from in situ TUNEL, ISEL, and ISOL reactions. Am J Clin Pathol 2004;121:108–16.
19. Fridman JS, Parsels J, Rehemtulla A, Maybaum J. Cytochrome c depletion upon expression of Bcl-XS. J Biol Chem 2001;276:4205–10.
20. White RL, Wittenberg BA. Mitochondrial NAD(P)H, ADP, oxidative phosphorylation, and contraction in isolated heart cells. Am J Physiol Heart Circ Physiol 2000;279:H1849–57.
21. Stanley WC, Chandler MP. Energy metabolism in the normal and failing heart: potential for therapeutic interventions. Heart Fail Rev 2002;7:115–30.
22. Plas DR, Talapatra S, Edinger AL, Rathmell JC, Thompson CR. Akt and Bcl-xl promote growth factor independent survival through distinct effects on mitochondrial physiology. J Biol Chem 2001;276:12041–8.
23. Scorrano L, Oakes SA, Opferman JT, et al. BAX and BAK regulation of endoplasmic reticulum ca2+: a control point for apoptosis. Science 2003;300:135–9.
24. Lucas DT, Szweda LI. Cardiac reperfusion injury: aging, lipid peroxidation, and mitochondrial dysfunction. Proc Natl Acad Sci USA 1998;95:510–4.
25. Clem RJ, Cheng EH-Y, Karp CL, et al. Modulation of cell death by Bcl-xL through caspase interaction. Proc Natl Acad Sci USA 1998;95:554–9.
26. Suleiman MS, Halestrap AP, Griffiths EJ. Mitochondria: a target for myocardial protection. Pharm Ther 2001;89:29–46.
27. Kerr PM, Suleiman MS, Halestrap AP. Reversal of permeability transition during recovery of hearts from ischemia and its enhancement by pyruvate. Am J Physiol 1999;276:H496–502.
28. Minners J, McLeod CJ, Sack MN. Mitochondrial plasticity in classical ischemic preconditioning-moving beyond the mitochondrial KATP channel. Cardiovasc Res 2003;59:1–6.
29. Garland JM, Halestrap A. Energy metabolism during apoptosis. Bcl-2 promotes survival in hematopoietic cells induced to apoptose by growth factor withdrawal by stabilizing a form of metabolic arrest. J Biol Chem 1997;272:4680–8.
30. Zhao YY, Sawyer DR, Baliga RR, et al. Neuregulins promote survival and growth of cardiac myocytes. Persistence of ErbB2 and ErbB4 expression in neonatal and adult ventricular myocytes. J Biol Chem 1998;273:10261–9.
31. Wencker D, Chandra M, Nguyen K, et al. A mechanistic role for cardiac myocyte apoptosis in heart failure. J Clin Invest 2003;111:1497–504.
32. Elsasser A, Suzuki K, Lorenz-Meyer S, Bode C, Schaper J. The role of apoptosis in myocardial ischemia: a critical appraisal. Basic Res Cardiol 2001;96:219–26.
33. Scheubel RJ, Bartling B, Simm A, et al. Apoptotic pathway activation from mitochondria and death receptors without caspase-3 cleavage in failing human myocardium: fragile balance of myocyte survival? J Am Coll Cardiol 2002;39:481–8.
34. Narula J, Arbustini E, Chandrashekhar Y, Schwaiger M. Apoptosis and the systolic dysfunction in congestive heart failure. Story of apoptosis interruptus and zombie myocytes. Cardiol Clinics 2001;19:113–26.